Intrinsic chirp of attosecond pulses: Single-atom model versus experiment

S. Kazamias* and Ph. Balcou
Laboratoire d'Optique Appliquée, ENSTA-Ecole Polytechnique, CNRS UMR 7639, F-91761 Palaiseau cedex, France
(Received 4 July 2003; published 30 June 2004)

We demonstrate and evaluate the importance of an intrinsic chirp inherent to attosecond pulse creation accompanying high-order harmonic generation in recently published experimental data by Dinu *et al.* [Phys. Rev. Lett. **91**, 063901 (2003)]. We present an analytical model, from which the atomic origin of the harmonic chirp is clearly understood. Moreover, the behavior of the chirp as a function of experimental parameters such as laser intensity is inferred. The comparison between our model and the experimental data provides us with useful information about the conditions in which the high-order harmonics is generated.

DOI: 10.1103/PhysRevA.69.063416 PACS number(s): 32.80.Rm, 42.65.Ky

I. INTRODUCTION

The ability to create and measure light pulses in the attosecond (as) range is one of the recent exciting developments of extreme nonlinear optics, occurring when atoms and molecules are submitted to strong laser fields. Theoretical predictions of attosecond pulses were presented by Farkas and Toth [1], and Antoine *et al.* [2]. Experimentally, a few methods have been pursued in parallel to create and measure such attosecond pulses: Harris *et al.* [3] take advantage of high-order Raman processes in molecular gases; different experiments performed by Haentschel *et al.* in Vienna have indicated the existence of isolated pulses of 650 as, resulting from high-order harmonic generation in neon in a particular, carrier-phase-dependent harmonic generation regime [4].

An important breakthrough for the study of attosecond physics in high-order harmonic generation (HHG) was performed in Ref. [5] by the first measurement based on the so-called RABBITT method (Resolution of Attosecond Beating By Interference of Two-photon Transitions) [6] of the relative phases between five harmonic orders generated in an argon gas jet by a 30-fs laser pulse (11-optical-cycle FWHM). It allowed the conclusion that the interference of harmonics 11 to 19 would lead to the generation of a train of attosecond pulses occurring twice per optical cycle of the fundamental infrared radiation (2.6 fs) and whose duration is equal to 250 as.

Up to now, characterization studies of attosecond pulses have concentrated on the measurement of the duration of each pulse, based, e.g., on autocorrelation techniques [7], such as the recent work by Tzallas *et al.* that led to the characterization of 780-as duration pulses for the interference of 5 harmonic orders [8]. However, a major advantage of the RABBITT method is the ability to recover the full temporal profile of the attosecond pulses. In particular, any chirp effect could be characterized.

From a theoretical point of view, high-order harmonic generation is well understood in the three-step model paradigm [9,10]. A simplified view of the phase behavior of high-order harmonic is often derived from this model; however, as was emphasized by Salières *et al.* [11] and Kim *et al.* [12], each high-order harmonic actually has a complicated phase behavior, leading for instance to a chirp on the time scale of the laser pulse duration. A different kind of chirp may be expected to occur on each attosecond burst generated at a laser half-cycle. This attosecond chirp will be related to the phases of several harmonics relative to one another.

The aim of this paper is to revisit recent experimental data that show the existence of an intrinsic chirp of high-order harmonics, and to explain it in the simple approach of the semiclassical, three-step model. Quite simple analytical formulas can be derived, that will be used to discuss the data. The predictions that can be made using this model are in good agreement with the results obtained recently both experimentally and theoretically by Mairesse *et al.* (CEA Saclay group) [13] and Kim *et al.* (KAIST group) [14].

II. ATTOSECOND PULSE CHIRP MEASUREMENT WITH THE RABBITT METHOD

A. Attosecond chirp definitions

The RABBITT method [6] is a powerful way to evaluate the value of the spectral phase for a set of consecutive harmonics by measuring the electronic spectra obtained by the ionization of a rare gas in the presence of harmonic radiation and a small part of the fundamental infrared laser. The electronic spectra show important peaks for the kinetic energies corresponding to the absorption of energy of one harmonic photon. Sidebands also exist that correspond to the simultaneous absorption of one harmonic photon plus the absorption or emission of one infrared photon. A given electronic energy in a sideband may be the result of different processes: first, the absorption of one infrared photon and one qth-order harmonic photon, second the emission of one infrared photon and the absorption of one $(q+2)$th-order harmonic photon. The sideband amplitude is thus the result of the quantum interference between those two quantum paths that lead to the same final state. By studying the sideband amplitude as a function of the delay between the infrared and harmonic photon beams, the RABBITT method provides the harmonic phase values desired.

*Present address: Laboratoire d'Interaction du rayonnement X Avec la Matière de l' Université Orsay Paris XI, CNRS UMR 8624, F-91405 Orsay Cedex, France

A recent Letter [15] extended the RABBITT method by performing a thorough analysis of all experimental phases incurred by high-order harmonics. The authors were able to determine the subcycle timing of attosecond XUV bursts regarding the infrared optical cycle. The major result was that the attosecond pulse is emitted 1410 as after one maximum of the laser field. The attosecond burst duration was the result of the interference of the five harmonics 11 to 19 and was found to be 266 as, which is close to the Fourier transform value given by $\delta t = T/2N$, where N is the number of interfering harmonic orders and T the infrared optical period (2.67 fs for an 800-nm laser beam).

This limit is only obtained in the case when the attosecond pulse is not chirped, implying that all harmonic orders are emitted at the same time t, as was assumed in Refs. [5,15]. An attosecond pulse will be chirped if the various frequency components are delayed linearly in time. The most convenient definition to characterize the chirp in the single-atom process of high harmonic generation is therefore

$$C = \frac{\partial t}{\partial \omega_{\mathrm{HHG}}} = \frac{\partial^2 \phi}{\partial \omega_{\mathrm{HHG}}^2}, \tag{1}$$

where ω_{HHG} is the harmonic pulsation and ϕ is the harmonic phase. Following this definition, $C=0$ means a perfectly linear behavior of the harmonic phases as a function of the order, thus no chirp for the attosecond bursts. C will be expressed in as/eV so that the difference in recombination times between two harmonic orders q_1 and q_2 will simply be given by

$$\Delta t(\mathrm{as}) = 1.5C(q_1 - q_2), \tag{2}$$

where 1.5 eV is the energy of one infrared photon of the pump laser ($\lambda = 800$ nm). Moreover, the maximum recombination time difference between N interfering harmonic orders will be

$$\Delta t(\mathrm{as}) = 3C(N-1). \tag{3}$$

The influence of this chirp on the attosecond burst duration can be evaluated by comparing the former value to $\delta t = T/2N$, which is the ultimate limit of attosecond burst duration in a nonchirped case. As a consequence, the following condition on C must be fulfilled in order to neglect the chirp effect:

$$C(\mathrm{as/eV}) \ll \frac{400(\mathrm{as/eV})}{N(N-1)}. \tag{4}$$

Note that the commonly used definition of the chirp in laser physics especially for CPA (chirped pulse amplification) high-power laser systems is $\Gamma = \partial\omega/\partial t$ and is expressed in fs^{-2}. $\partial t/\partial\omega$ in that case is called "group delay dispersion."

The link between those two definitions of chirp is

$$\Gamma(\mathrm{fs}^{-2}) = \frac{1516}{C(\mathrm{as/eV})}. \tag{5}$$

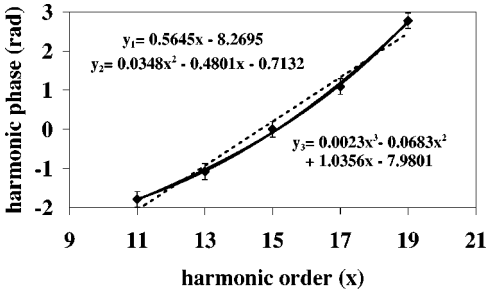

FIG. 1. Full diamonds: relative harmonic phases generated in argon with a 10^{14}-W/cm^2 laser intensity for orders 11 to 19 measured experimentally in Ref. [2]; dotted line: linear fit; full line: polynomial third-order fit from which the second order fit cannot be graphically distinguished here.

B. Method of chirp analysis

We performed a deeper analysis of the phase behavior published in Ref. [15]. The time analysis in this work was performed with a linear fit of the harmonic phases as a function of frequency. In order to extract higher orders of the dispersion, and in particular the chirp, it is necessary to resort to fits of higher polynomial orders. We thus present in Fig. 1 the comparison between a linear fit (dotted line) and a second- or third-order polynomial regression (thick line). The phase behavior is clearly not linear, indicating a complex chirp behavior. Graphically, the difference between the second- and third-order fits is quite small with respect to the experimental error bars. The chirp coefficient extracted from those differing fits is identical to within a few percent for the center band harmonic, and reaches maximum values of 50% for the high-order harmonics at the edges of the plateau region in the experimental conditions considered here.

Figure 2 presents the recombination times inferred from the three polynomial fits of increasing order: from linear (dotted line) to second-order (black squares) and third-order (thick line) ones. The quadratic phase fit leads to a constant chirp C equal to 20 as/eV ($\Gamma = 76\ \mathrm{fs}^{-2}$). The recombination time difference between H11 and H19, that corresponds to a 12-eV photon energy difference, is thus 236 as. This experimental value of the chirp has to be compared to the total burst duration, whose estimated value is only slightly higher

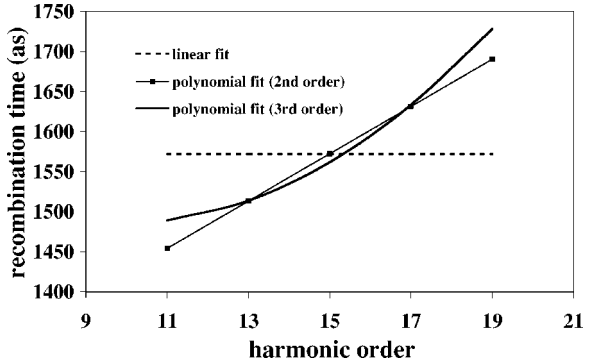

FIG. 2. Recombination times for harmonic orders 11 to 19 inferred from Fig. 1; dotted line: linear fit; full squares: second-order polynomial fit; thick line: third order.

(266 as). This result shows that the importance of the chirp for the generation of attosecond bursts must not be neglected in that experimental case.

We now present a simple theoretical model that allows one to understand the origin of the chirp and to numerically evaluate its influence.

III. ATTOSECOND CHIRP ANALYSIS IN THE SEMICLASSICAL THREE-STEP MODEL

A. Origin of the chirp

The most efficient way to describe the process of high-order harmonic generation (HHG) in rare gases by an intense laser field is the semiclassical "three-step model" [9,10]. In this model, the electron is first tunnel ionized by the strong electric field of the linearly polarized fundamental laser. It is then accelerated by the electric field and may at last recombine with its parent ion and emit a harmonic photon, whose energy is the sum of the ionization potential of the generating gas and the electron kinetic energy gain.

This first model was generalized in a full quantum theoretical frame by Lewenstein *et al.* in Ref. [16] and was later confirmed by the use of the Feynman's path-integral approach that allows one to understand the interaction between a strong laser field and an atom [17]. A key result of the quantum Lewenstein model is the semiclassical interpretation: a saddle-point analysis shows that the dominant quantum paths follow the classical trajectories in the continuum. It was shown that the electron trajectories that contribute the most to the harmonic emission are those for which the electron is emitted in the continuum without any initial velocity. The second important feature was the existence of two different quantum paths (electron trajectories) that lead to the same kinetic energy gain [18]: the shorter one is also called the first quantum path, the longer one the second.

The saddle-point method allows one to discuss many physical features from a classical standpoint. It is in particular possible to compute the electron position and velocity along a given trajectory. In the following, we will denote $t'$the time at which the electron is emitted in the continuum. The laser field is defined as $E(t)=E_0\cos(\omega t)$, where ω is the laser pulsation $(2.35\times10^{15}\ \mathrm{rad\ s^{-1}})$. The electron motion equations can be analytically solved and give for the velocity $v=0$and distance$x=0$ to the parent ion

$$v(t)=\frac{qE_0}{m\omega}[\sin(\omega t)-\sin(\omega t')], \tag{6}$$

$$x(t)=-\frac{qE_0}{m\omega^2}[\cos(\omega t)-\cos(\omega t')]-\frac{qE_0}{m\omega}\sin(\omega t')(t-t'), \tag{7}$$

where q and m are the electronic charge and mass, respectively. Note that we used the initial conditions $v(t')=0$ [16] and $x(t')=0$.

If the electron recombines at a time t (condition $x=0$), the harmonic photon energy will be

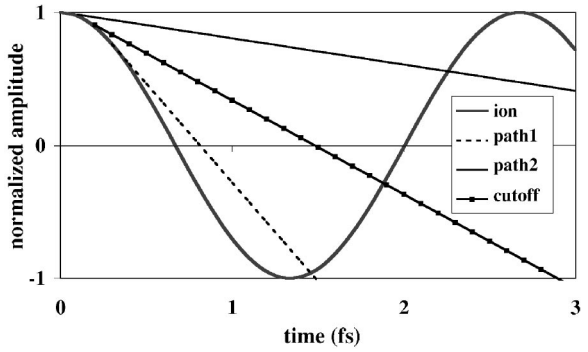

FIG. 3. Ion (thick gray line) and electron trajectories for the first and second quantum path corresponding to a 10-eV kinetic energy gain (dotted line and full line, respectively). The cutoff trajectory is represented by the full squares.

$$q\hbar\omega=I_p+2U_p[\sin(\omega t)-\sin(\omega t')]^2, \tag{8}$$

where I_p is the ionization potential and U_p the laser ponderomotive energy proportional to the laser intensity $[U_p=(qE_0)^2/4m\omega^2]$.

A harmonic trajectory analysis is easier to perform in an oscillating referential designed so that the electron trajectory is reduced to a linear motion $(x_{\mathrm{elec}}(t)=(qE_0/m\omega^2)[\cos(\omega t')]-(qE_0/m\omega)\sin(\omega t')(t-t'))$ and for which the parent ion is no more the static reference $(x=0)$ but periodically oscillates $(x_{\mathrm{ion}}(t)=(qE_0/m\omega^2)[\cos(\omega t)])$ [19]. The condition $v(t')=0$ is represented here by the fact that the ionic and electronic trajectories are tangential at the ionization time. As can be deduced from Eqs. (7) and (8), the kinetic energy gain will then be proportional to the square of the slope difference between the two trajectories at the recombination time.

Those trajectories are represented in Fig. 3. We chose three different cases typical of the high-order harmonic generation process: the black squares represent the trajectory that leads to the maximum kinetic energy gain and thus the highest harmonic order q, also called "cutoff order." The latter is given by the well-known law: $q_{\max}=(I_p+3.17U_p)/\hbar\omega$ that can be deduced from the above formulas. For smaller harmonic orders, there exist two recombination times that lead to the same gain. The first one corresponds to later ionization but earlier recombination times than the second one. It is logically called the short quantum path or "path 1." Dotted and full lines represent the first and second quantum path, respectively, both corresponding to a 10-eV kinetic energy gain if we consider a 10^{14}-W/cm^2 laser intensity. It is graphically visible that the kinetic energy gain increases with the recombination time along the first quantum path, and decreases after the cutoff point for the second quantum path (upper part of the curve).

Figure 4 represents the recombination time t computed from the three-step model as a function of the harmonic order and for different laser intensities. The rising part of each curve corresponds to the first quantum path; then, the cutoff order is clearly visible and depends on the laser intensity. The decreasing part corresponds to the second quantum path for which the chirp becomes negative. As was shown in Ref.

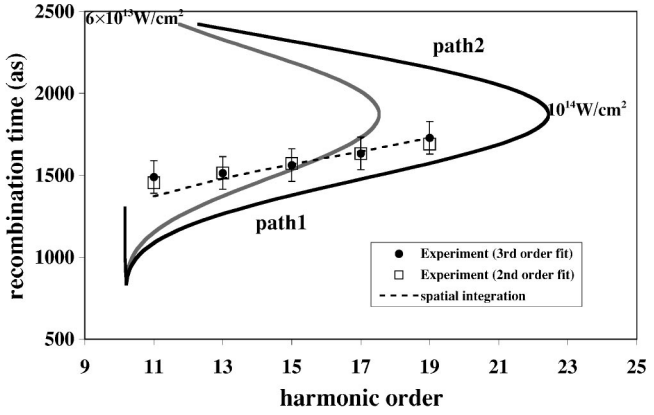

FIG. 4. Recombination time as a function of the harmonic order generated in argon for different laser intensities (gray line: 6×10^{13} W/cm^2, black line: 10^{14} W/cm^2); full circles: experimental points inferred using a third-order fit with 100-as error bars; black squares: the same but considering the second-order fit; dotted gray line: theoretical calculation from a spatial integration.

[15] and within the experimental uncertainty on the time evaluation of about 100 as, the experimental values of the phases are typical of the first quantum path. This result confirms the work of Ref. [20] that showed that the first quantum path was the best candidate for a proper phase locking for the generation of attosecond bursts. The experimental chirp sign there is another confirmation of this prediction.

B. Analytical computation of the chirp value

Within the framework of the semiclassical model detailed above, the harmonic chirp can be evaluated through the combination of Eqs. (7) and (8).

In order to determine the harmonic chirp defined as $\partial t/\partial\Delta E$, where ΔE is the kinetic energy gain, we introduce an auxiliary function $F(t,\Delta E)$

$$F(t,\Delta E)=\cos(\omega t)-\sqrt{1-\left(\sin(\omega t)+\sqrt{\frac{\Delta E}{2U_p}}\right)^2}+\left(\omega t-\sin^{-1}\left(\sin(\omega t)+\sqrt{\frac{\Delta E}{2U_p}}\right)\right)\times\left(\sin(\omega t)+\sqrt{\frac{\Delta E}{2U_p}}\right), \quad (9)$$

that corresponds to the ion /electron separation and has to obey $F(t,\Delta E)=0$ at the recombination time, as can be seen from Eqs. (7) and (8).

Using the fact that $\partial t/\partial\Delta E=-(\partial F/\partial\Delta E)/(\partial F/\partial t)$, the chirp C can be calculated and finally expressed as the following:

$$C(\Delta E)=\frac{-(t-t')}{\sqrt{8U_p\Delta E}\left(\sqrt{\frac{\Delta E}{2U_p}}+\omega\cos(\omega t)(t-t')\right)}. \quad (10)$$

The chirp value is represented in Fig. 5 for different laser intensities. It appears clear that the chirp decreases with the intensity: it is approximately equal to 30 as/eV for

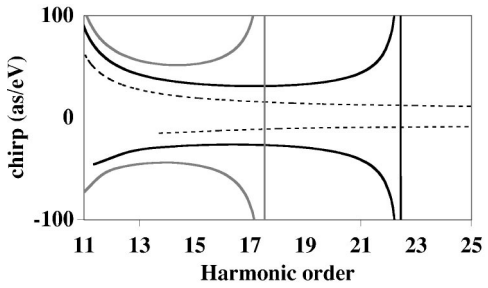

FIG. 5. Harmonic chirp as a function of the harmonic order for different laser intensities (gray line: 6×10^{13} W/cm^2; black line: 10^{14} W/cm^2; dotted line: 3×10^{14} W/cm^2).

10^{14} W/cm^2 and is reduced to 15 as/eV for 3×10^{14} W/cm^2. We also note from Fig. 5 that the chirp value is quite constant in the plateau region defined as the harmonic orders between the perturbative regime ($q\hbar\omega\leqslant I_p$) and the cutoff region. At the edges of that domain the chirp and harmonic phases strongly diverge and the simple approach is no longer valid, implying the need for higher orders in the description of the phase frequency behavior.

IV. SPATIAL INTENSITY EFFECT ON THE CHIRP

The most interesting information about the harmonic emissive zone is obtained by the comparison between experimental values (black diamonds in Fig. 4) and those from the calculations at various laser intensities. The effective laser intensity at focus is indeed very difficult to estimate experimentally [21], and 10^{14} W/cm^2 could appear to be slightly overestimated for the generation conditions of Ref. [15]: considering H19 alone, the agreement between the experimental and theoretical recombination times would be better if $I=8\times10^{13}$ W/cm^2, and for H15 if $I=6\times10^{13}$ W/cm^2. Moreover, the experimental chirp value turns out to be much smaller than what is inferred at any fixed laser intensity for all harmonic orders.

This is illustrated in Fig. 6, which displays the recombination times as a function of the laser intensity for the harmonic orders 11 to 19. The direct comparison with experimental points (full circles) already shows that the effective

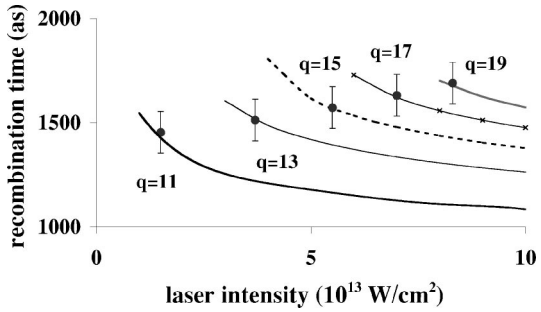

FIG. 6. Recombination time as a function of the laser intensity for the harmonic orders between 11 and 19 calculated from the three-step model (various lines). The experimental values are represented by the full circles; the estimated uncertainty is 100 as.

intensity required by each harmonic to fit the experimental data increases with the order. We suggest that this effect arises from macroscopic volume effects, akin to those analyzed by Gaarde and Schafer in their phase-locking studies depending on the quantum paths [20].

In a simple approach, we model the experimental recombination time (frequency derivative of the measured phase) that is bound to arise from a RABBITT measurement, as the recombination time averaged over the laser beam section in the emission region.

We assume a Gaussian form for the laser focus intensity I as a function of the distance r to the axis

$$I(r) = I_0 e^{(-2r^2/w_0^2)}. \tag{11}$$

The maximum intensity on axis is called I_0 and w_0 is the laser waist.

The intensity decreases with r down to a radial cutoff value, noted as r_{cutoff}, for which the intensity experienced by the atoms far from the axis is exactly the cutoff intensity at a given harmonic order

$$r_{\text{cutoff}}^2 = \frac{w_0^2}{2} \ln\left(\frac{I_0}{I_{\text{cutoff}}}\right). \tag{12}$$

The averaged recombination time for a given harmonic order will then be

$$t_{\text{av}} = \frac{\int_{r=0}^{r_{\text{cutoff}}} t(I_0 e^{(-2r^2/w_0^2)}, q) 2\pi r \, dr}{\pi r_{\text{cutoff}}^2}. \tag{13}$$

This expression can be considerably simplified by making a change of variable, that leads to

$$t_{\text{av}} = \frac{1}{\ln\left(\frac{I_0}{I_{\text{cutoff}}}\right)} \int_{I_{\text{cutoff}}}^{I_0} t(I) dI/I. \tag{14}$$

The last equation indicates that the spatial region that plays a major role for each harmonic order is the zone for which the intensity is as small as possible ($I \simeq I_{\text{cutoff}}$), corresponding to a large cross-sectional area. As an illustration, a reasonable agreement between theory and the experimental points is roughly obtained by considering the recombination time for each harmonic order at the intensity for which the next order enters the plateau region [$I_{\text{cutoff}}(q+1)$]. More precisely, the dotted gray line in Fig. 4 represents the full calculation from Eq. (14). The agreement between experimental and theoretical points in that case is very good with respect to experimental uncertainty, better than 100 as. We emphasize that the current simple model involves no adjustable parameter.

It is striking that the spatial intensity effect in the experimental case of Ref. [15] tends to reduce the harmonic chirp and favor the generation of shorter attosecond bursts, as measured with the RABBITT method. Propagation effects may therefore play a beneficial role in the characteristics of attosecond pulses generated in a macroscopic medium, in the specific case when the attosecond bursts are used or measured in the far field of the harmonic beam.

The macroscopic effects discussed here should play a lesser role in other experimental conditions, especially when the intensity is higher, so that the span of high-order harmonics considered is a much smaller fraction of the total plateau extent. The recombination time variation with intensity tends to zero at high intensities (as can be seen in Fig. 6) so that predictions of the single-atom model provide a better approximation to the measured chirp value [13].

V. CONCLUSION

In summary, we have shown that the attosecond bursts inherent to the process of high-order harmonic generation at the atomic scale should display important chirp values. The contribution of the first quantum path should have a positive chirp, while that of the second one should be negative. These characteristics do not strongly depend on the nature of the generating gas, but are directly related to the laser intensity. Those single-atom predictions are in qualitative agreement with the data published in Ref. [15], and more precisely allow discrimination between the first and second quantum paths. The values inferred from the calculations are nevertheless higher than those measured. This is most probably related to a three-dimensional intensity smoothing in the experimental case, as indicated by the much better quantitative agreement with the data, when the chirp values are computed for each harmonic as an average on all intensities experienced on axis but also far from the axis. Our single-atom model should therefore be complementary to a full coupled atomic and propagation study along the lines proposed by Milosevic *et al.* [22]. This could help to explain why such ultrashort attosecond pulses are actually observed experimentally, in spite of the temporal and spatial blurring effects.

ACKNOWLEDGMENTS

We want to thank H. G. Muller and C. Dinu from the FOM in Amsterdam and P. Agostini and P. Breger from CEA-Saclay (France) for fruitful collaboration on the experimental data and making the latter available prior to publication.

[1] G. Farkas and C. Toth, Phys. Lett. A **168**, 447 (1992).
[2] Ph. Antoine, A. L'Huillier, and M. Lewenstein, Phys. Rev. Lett. **77**, 1234 (1996).
[3] S. E. Harris, J. J. Macklin, and T. W. Hansch, Opt. Commun. **100**, 487 (1993).
[4] M. Haentschel, R. Kienberger, Ch. Spielmann, G. A. Reider, N. Milosevic, T. Brabec, P. B. Corkum, U. Heinzmann, M. Drescher, and F. Krausz, Nature (London) **414**, 511 (2001).

[5] P. M. Paul, P. Breger, P. Agostini, E. S. Toma, H. G. Muller, G. Mullot, F. Augé, and Ph. Balcou, Science **292**, 1689 (2001).
[6] H. G. Muller, Appl. Phys. B: Lasers Opt. **B74**, S17 (2002).
[7] N. A. Papadogiannis, L. A.A. Nikolopoulos, D. Charalambidis, G. D. Tsakiris, P. Tzallas, and K. Witte, Appl. Phys. B: Lasers Opt. **76**, 721 (2003).
[8] P. Tzallas, D. Charalambidis, N. A. Papadogiannis, K. Witte, and G. D. Tsakiris, Nature (London) **426**, 267 (2003).
[9] K. C. Kulander, K. J. Schafer, and J. L. Krause, in *Proceedings of the Super Intense Laser-Atom Physic III Workshop*, Vol. 316 of NATO Advanced Study Institute, Series B: Physics (Plenum Press, New York, 1993).
[10] P. B. Corkum, Phys. Rev. Lett. **71**, 1994 (1993).
[11] P. Salières, Ph. Antoine, A. de Bohan, and M. Lewenstein, Phys. Rev. Lett. **81**, 5544 (1998).
[12] J. H. Kim, D. G. Lee, H. J. Shin, and C. H. Nam, Phys. Rev. A **63**, 063403 (2001).
[13] Y. Mairesse, A. de Bohan, L. J. Frasinski, H. Merdji, P. Monchicourt, P. Breger, M. Kovacev, B. Carré, H. G. Muller, P. Agostini, and P. Salières, Science **302**, 1540 (2003).
[14] K. T. Kim, C. M. Kim, K-H. Hong, D. G. Lee, M-G. Baik, and C. H. Nam, WB6 technical digest of the conference, "Applications of High Field and Short Wavelength Sources X" (HFSW X) (2003).
[15] L. C. Dinu, H. G. Muller, S. Kazamias, G. Mullot, F. Augé, Ph. Balcou, P. M. Paul, M. Kovacev, P. Breger, and P. Agostini, Phys. Rev. Lett. **91**, 063901 (2003).
[16] M. Lewenstein, Ph. Balcou, M. Y. Ivanov, A. L'Huillier, and P. B. Corkum, Phys. Rev. A **49**, 2117 (1994).
[17] P. Salières, B. Carré, L. Le Déroff, F. Grasbon, G. G. Paulus, H. Walther, R. Kopold, W. Becker, D. B. Milosevic, A. Sanpera, and M. Lewenstein, Science **292**, 902 (2001).
[18] M. Lewenstein, P. Salières, and A. L'Huillier, Phys. Rev. A **52**, 4747 (1995).
[19] H. G. Muller and F. C. Kooiman, Phys. Rev. Lett. **81**, 1207 (1998).
[20] M. B. Gaarde and K. J. Schafer, Phys. Rev. Lett. **89**, 213901 (2002).
[21] S. Kazamias, F. Weihe, D. Douillet, C. Valentin, T. Planchon, S. Sebban, G. Grillon, F. Augé, D. Hulin, and Ph. Balcou, Eur. Phys. J. D **21**, 353 (2002).
[22] N. Milosevic, A. Scrinzi, and Th. Brabec, Phys. Rev. Lett. **88**, 093905 (2002).